Modeling and numerical simulation of argon and hydrogen plasma sheaths with secondary electron emission

Aziza Asserghine[1*] and *Fatiha* Maaroufi[1]

[1]LPTPME, Department of Physics, Faculty of Sciences, Mohammed First University, Oujda, Morocco

Abstract. The characteristics of plasma sheaths in different background gases are of great importance for understanding plasma-surface interactions. In this work, a comparative investigation is performed on argon and hydrogen thermal electropositive plasmas containing primary electrons and singly charged ions near an electron-emitting surface. By taking into account the wall potential condition and the modified Bohm criterion, the plasma sheath characteristics such as the spatial profiles of secondary electron density and electrostatic potential are numerically investigated for argon and hydrogen plasmas with non-Maxwellian and Maxwellian primary electron distributions. This study provides valuable insights into plasma-surface interactions and may be useful in applications such as plasma processing and fusion technologies.

Keywords: Plasma sheath, Plasma–surface interactions, Argon and hydrogen plasmas, Electron emission, Non-Maxwellian distributions

1 Introduction

The contact between plasma and a material wall lead to the formation of a thin non neutral layer, known as the sheath. Because of the higher mobility of electrons compared with ions, the electrons reach the wall more rapidly, leaving a region enriched with ions. This charge imbalance generates an electric field that drives ions toward the wall while electrons are repelled. The sheath plays an essential role in numerous applications, including plasma processing [1], electric propulsion [2], and interactions between plasma and reactors in fusion devices [3]. For example, in material processing, plasma sheaths are exploited to control ion bombardment and tailor surface properties in technologies relevant to renewable energy devices, including the fabrication of bulk and thin film silicon photovoltaic cells [4].
A particularly important mechanism in sheath physics is secondary electron emission (SEE), in which energetic ions or primary electrons impacting the surface release additional electrons. Numerous investigations have reported that these secondary electrons can

* Corresponding author: a.asserghine@ump.ac.ma

significantly modify the sheath potential drop and overall sheath structure [5-7], making SEE widely studied due to its importance a broad range of plasma systems, from Hall thrusters [8] to magnetic confinement fusion devices [9].

Most classical sheath studies consider plasma electrons to obey a Maxwell-Boltzmann distribution [10-14]. However, a large number of experimental and theoretical results [15-17] have demonstrated that the Boltzmann Gibbs statistics fail to accurately describe systems in which long range Coulomb forces and nonequilibrium effects are present. The q-nonextensive formalism introduced by Tsallis [18] provides a generalized statistical description for systems with long range interactions through the nonextensive parameter q. This parameter characterizes the deviation from the Maxwellian behaviour, where $q < 1$ corresponds to superextensive electron populations, whereas $q > 1$ corresponds to subextensive distributions. The nonadditive Tsallis entropy reduces to the classical Boltzmann-Gibbs entropy in the limit $q \to 1$. Many studies have examined how the nonextensive parameter affects sheath properties such as potential profiles and charged particles densities, under different plasma conditions [19-21].

Superextensive electron populations $(q < 1)$ contain in particular a larger number of energetic electrons and therefore exhibit a greater ability to generate secondary electron emission (SEE). For this reason, particular attention is given to the case $q < 1$ in the present work, while comparing it to the Maxwellian distribution.

In our previous study [20], we investigated the impact of the non-extensive parameter and secondary electron emission on the sheath properties in argon plasma. In the present work, we extend the analysis by comparing plasmas composed of heavy ions and light ions under both superextensive and Maxwellian primary electron distributions, while examining the effect of positive ion temperature and SEE generated by positive ions and primary electrons. This comparative approach allows us to clarify how ion mass affects the sheath properties, which is an aspect that has not been examined previously in the presence of SEE.

This paper is structured into four sections, with the Introduction presented in Sec.1. In Sec. 2, we present the basic equations describing our plasma model. In Sec. 3, we discuss the numerical results obtained. A summary of the main conclusions is given in Sec.4.

2 Theoretical model

In this work, we investigate a collisionless, unmagnetized plasma sheath composed of primary electrons, thermal positive ions, and secondary electrons emitted from the wall due to the impact of both ions and primary electrons. The region of interest extends from the quasineutral plasma $(x < 0)$ to the nonneutral sheath, where the sheath edge is taken at $(x = 0)$. At this position, the quasineutrality condition is satisfied, $n_{e0} + n_{s0} = n_{i0}$, where n_{e0}, n_{s0}, and n_{i0} denote the primary electron, secondary electron, and positive ion densities at the sheath edge $(x = 0)$, respectively.

The primary electrons obey a nonextensive distribution [21], and their density is expressed as

$$n_e = n_{e0} \left[1 + (q-1)\frac{e\phi}{k_B T_e}\right]^{\frac{q+1}{2(q-1)}} \qquad q \neq 1 \qquad (1)$$

where q represents the degree of nonextensivity and T_e denotes the electron temperature.

For $q = 1$, the distribution simplifies to the classical Maxwell-Boltzmann distribution, and the primary electron density becomes

$$n_e = n_{e0}\, exp\left(\frac{e\phi}{k_B T_e}\right) \qquad (2)$$

The thermal positive ions and secondary electrons are considered as fluids in the steady state and are governed by the following equations.

Continuity equations:

$$\frac{\partial(n_i\,v_i)}{\partial x}=0 \tag{3}$$

$$\frac{\partial(n_s\,v_s)}{\partial x}=0 \tag{4}$$

Momentum conservation equations:

$$m_i v_i\,\frac{\partial v_i}{\partial x}=-e\,\frac{\partial\phi}{\partial x}-\frac{k_B T_i}{n_i}\frac{\partial n_i}{\partial x} \tag{5}$$

$$v_s\,\frac{\partial v_s}{\partial x}=\frac{e}{m_e}\,\frac{\partial\phi}{\partial x} \tag{6}$$

where m_e, v_s and n_s represent the mass, velocity, and density of secondary electrons, while n_i, v_i , m_i , and T_i correspond to the ion density, velocity, mass, and temperature. e denotes the elementary charge, and ϕ is the electrostatic potential.
The electrostatic potential satisfies Poisson's equation:

$$\frac{\partial^2\phi}{\partial x^2}=\frac{-e}{\varepsilon_0}(n_i-n_e-n_s) \tag{7}$$

where ε_0 is the electric permittivity of free space.
To normalize the governing equations, we define the following dimensionless variables:
$\Psi=\frac{-e\phi}{k_B T_e}$, $\xi=\frac{x}{\lambda_D}$, $u_{j=i,s}=\frac{v_j}{c_s}$, $c_s=\sqrt{\frac{k_B T_e}{m_i}}$, $N_{j=i,e,s}=\frac{n_j}{n_{i0}}$, $\lambda_D=\sqrt{\frac{\varepsilon_0\,k_B T_e}{n_{i0}\,e^2}}$, $\mu=\frac{m_i}{m_e}$, $T=\frac{T_i}{T_e}$
The normalized governing equations are

$$\frac{\partial(N_s\,u_s)}{\partial\xi}=0 \tag{8}$$

$$u_s{}'=-\frac{\mu}{u_s}\Psi' \tag{9}$$

$$\frac{\partial(N_i\,u_i)}{\partial\xi}=0 \tag{10}$$

$$u_i{}'=\frac{u_i}{u_i{}^2-T}\Psi' \tag{11}$$

$$N_e=N_{e0}(1-(q-1)\Psi)^{\frac{q+1}{2(q-1)}} \qquad q\neq 1 \tag{12}$$

$$N_e=N_{e0}\,exp\,(-\Psi) \qquad q=1 \tag{13}$$

$$\Psi''=N_i-N_e-N_s \tag{14}$$

Using the normalized continuity and momentum equations (Eqs. 9 and 10) and the zero net current condition i.e., the fluxes of ions and primary electrons reaching the wall are balanced by the flux of secondary electrons from the wall ($\Gamma_s=\gamma_e\,\Gamma_{ew}+\gamma_i\,\Gamma_{iw}$), we obtain

$$N_s=\frac{\gamma_e+\gamma_i}{1-\gamma_e}\frac{u_{i0}}{\sqrt{u_{sw}^2-2\mu(\Psi-\Psi_w)}} \tag{15}$$

where u_{sw} is the normalized secondary electrons velocity at the wall, u_{i0} is the positive ion velocity at the sheath edge, Ψ_w is the normalized floating potential at the wall. The coefficients γ_e and γ_i quantify the secondary electron emission from primary electrons and ions, respectively. The fluxes of positive ions and primary electrons reaching the wall are denoted by Γ_{iw} and Γ_{ew}.

3 Numerical results and discussions

To examine the combined effects of positive ions and secondary electron emission on the sheath properties, we numerically solved equations (10)-(15) using the fourth-order Runge-Kutta method for superextensive $(q<1)$ and Maxwellian $(q=1)$ primary electrons in argon and hydrogen plasmas. Following our previous work [20], the ion entrance velocity u_{i0} and the potential at the wall Ψ_w were determined numerically using the

Newton-Raphson method. Their analytical expressions are therefore not repeated here and can be found in Eqs. (21)-(22) and (27)-(28) of Ref.[20]. The boundary conditions at the sheath edge ($\xi = 0$) are $N_{e0} + N_{s0} = N_{i0}$, $\Psi_0 = 0$, and $\Psi_0{}' = 0.001$. The secondary electron velocity at the wall and the ion to electron mass ratios were taken as $u_{sw} = 40$, $\mu(Ar^+) = 7.333 \times 10^4$ and $\mu(H^+) = 1.851 \times 10^3$, respectively. The sheath region extends from $\xi = 0$ to the wall $\xi = \xi_w$, where the potential attains Ψ_w. Therefore, the thickness of the sheath is ξ_w.
We compare argon and hydrogen plasmas for both superextensive ($q = 0.6$) and Maxwellian ($q = 1$) primary electron distributions. For each plasma type, two secondary electron emission (SEE) cases are considered: (1) SEE due to primary electrons only ($\gamma_i = 0, \gamma_e = 0.7$), and (2) SEE generated by both ions and primary electrons ($\gamma_i = 0.4, \gamma_e = 0.7$). In all cases, the secondary electron density and the electrostatic potential are analyzed for three ion temperatures ($T = 0, 0.2, 0.4$).

3.1 Normalized secondary electron density

Considering secondary electron emission (SEE) from primary electrons only ($\gamma_i = 0$), Fig. 1 depicts the normalized secondary electron density N_s versus the normalized distance ξ from the sheath edge for both superextensive and Maxwellian primary electron distributions in argon (Ar) and hydrogen (H) plasmas. As shown in this Figure, an increase in the positive ion temperature T results in a higher secondary electron density. This means that in warm plasmas, the electrons emitted from the wall become more significant than in cold plasmas ($T = 0$), which is consistent with the enhanced ion flux reaching the wall. As T increases, positive ions acquire higher thermal energy, enabling a greater number to reach the sheath edge. This produces a larger ion flux toward the wall and consequently a higher secondary electron yield. Comparing Figs. 1a with 1a' and 1b with 1b', it is evident that the ion temperature has a stronger effect on N_s across the sheath in hydrogen plasma. In contrast, in argon plasma, the influence of ion temperature on N_s is mainly noticeable near the wall. Moreover, in hydrogen plasma (Figs. 1a' and 1b'), the effect of ion temperature on N_s is more pronounced for the Maxwellian primary electron distribution than for the superextensive case ($q = 0.6$). However, in argon plasma (Figs. 1a and 1b) the difference between Maxwellian and superextensive electrons remains very small. Regardless of the ion temperature and mass, the secondary electron density at the wall $N_{sw} = N_s(\xi = \xi_w)$ is slightly higher in the superextensive case compared to the Maxwellian one, while within the sheath region, the trend is inversed : Ns(Maxwellian)> Ns(superextensive). For a fixed ion temperature ($T = 0.4$) in superextensive distribution, the secondary electron density at the wall in argon plasma is $N_{sw}(Ar) = 0.06$, while in hydrogen plasma $N_{sw}(H) > 0.06$. The same behavior is observed for the Maxwellian distribution. This can be explained by the fact that lighter ions have higher mobility, allowing them to be more effectively accelerated through the sheath and to reach the wall with a higher flux compared to heavier ions, which enhances secondary electron emission. Furthermore, as the ion temperature decreases, the sheath region expands for both argon and hydrogen plasmas, irrespective of the primary electron distribution. This behavior is in agreement with the result obtained in Ref.[19] for a nonextensive plasma sheath with thermal ions and without SEE ($\gamma_i = \gamma_e = 0$). In addition, the sheath width in both argon and hydrogen plasmas is larger in the superextensive electron distribution, where electrons are more energetic, compared to the Maxwellian case. This result is consistent with those obtained in Ref.[19]. Moreover, when the positive ion mass decreases the sheath thickness decreases. Similar behaviors are also observed when positive ions contribute to SEE ($\gamma_i \neq 0$), as shown in Fig. 1. Comparing Figs. 1a and 1b with 2a and 2b, and also Figs. 1a' and 1b' with 2a' and 2b', it is seen that regardless of the background gas, primary electron distribution, and ion temperature, N_s

becomes larger when both ions and primary electrons contribute to SEE compared to SEE from primary electrons only. Moreover, including SEE from positive ions does not noticeably modify the sheath width, but the influence of ion temperature becomes more pronounced.

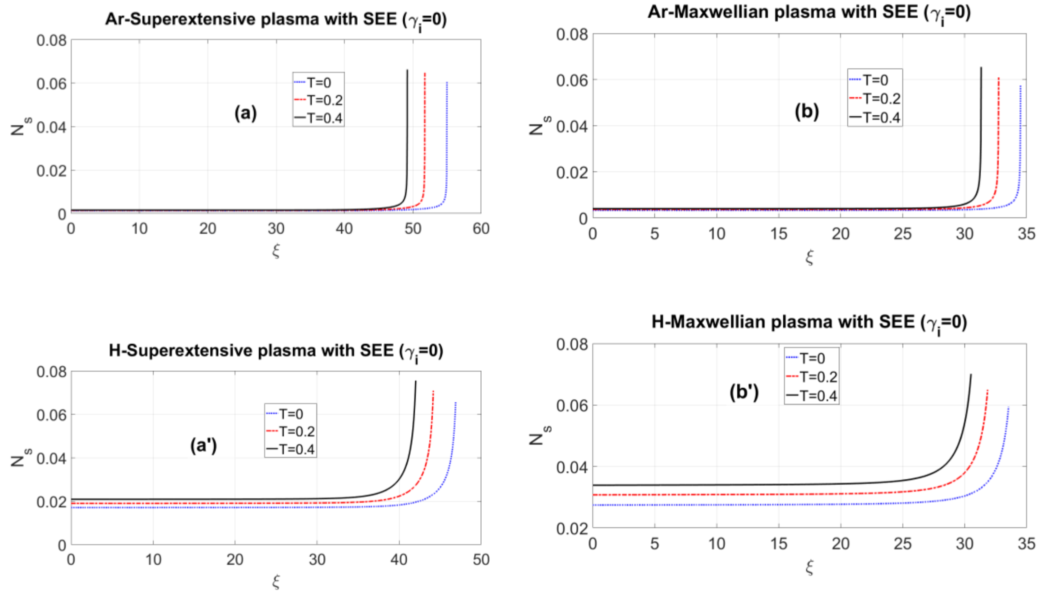

Fig. 1. Normalized secondary electron density versus ξ in superextensive and Maxwellian plasmas at different ion temperatures T, assuming SEE due to primary electrons only: (a) Argon plasma with superextensive electrons, (a') Hydrogen plasma with superextensive electrons, (b) Argon plasma with Maxwellian electrons, (b') Hydrogen plasma with Maxwellian electrons.

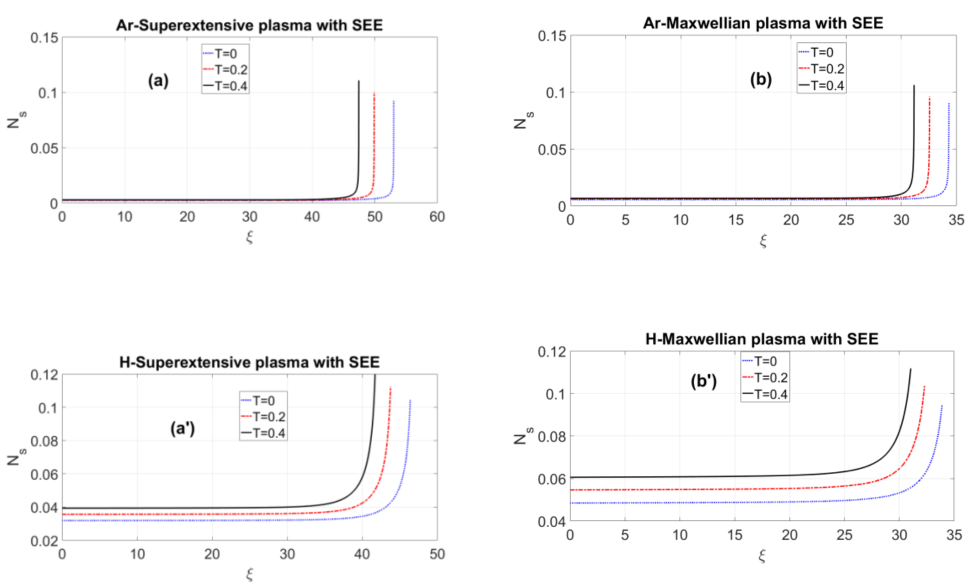

Fig. 2. Normalized secondary electron density versus ξ in superextensive and Maxwellian plasmas at different ion temperatures T with SEE: (a) Argon plasma with superextensive electrons, (a') Hydrogen plasma with superextensive electrons, (b) Argon plasma with Maxwellian electrons, (b') Hydrogen plasma with Maxwellian electrons.

3.2 Normalized electrostatic potential profile

Using the same boundary conditions and parameters described in Sec. 3.1, Figs. 3 and 4 present the normalized electrostatic potential across the sheath region for different values of the positive ion temperature T in argon (Ar) and hydrogen (H) plasmas, considering both the superextensive $(q = 0.6)$ and the Maxwellian $(q = 1)$ electron distributions. Two types of SEE are examined: SEE induced by primary electrons only $(\gamma_i = 0)$ and SEE produced by primary electrons and positive ions $(\gamma_i \neq 0)$. In the case of SEE from primary electrons only (Fig. 3), increasing the ion temperature raises the electrostatic potential throughout the sheath, whereas the sheath width contracts and the wall potential drop Ψ_w decreases. Warm ions have greater thermal velocities, which increases their flux toward the wall. This enhanced ion flux reduces the accumulation of positive charge in the sheath region, resulting in a reduction of Ψ_w. This behavior is in agreement with the findings of Ref. [22] for magnetized Maxwellian plasmas. For a fixed ion temperature, the potential is always larger for the superextensive distribution than for the Maxwellian one. Increasing the ion mass also leads to a higher potential across the sheath and at the wall. This effect is more pronounced in the superextensive case. A comparison between Figs.3 and 4 shows that including SEE from positive ions lowers the electrostatic potential at the wall in both gases, regardless of the ion temperature or the primary electron distribution. Ion impact at the wall generates additional emitted electrons, which partially compensates the positive space charge and therefore leads to a smaller potential drop at the wall. The ion induced SEE does not significantly affect the sheath thickness. This observation is consistent with the density profiles presented in Figs.1 and 2, where ion induced SEE increased the number of secondary electrons but had minimal impact on the spatial extent of the sheath.

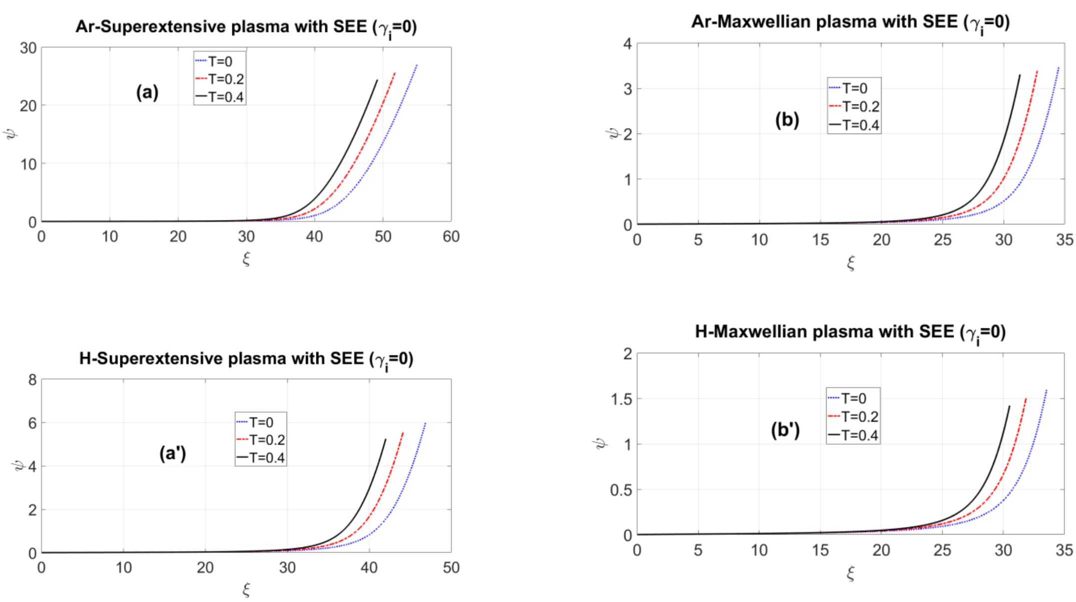

Fig. 3. Normalized potential versus ξ in superextensive and Maxwellian plasmas at different ion temperatures T, assuming SEE due to primary electrons only: (a) Argon plasma with superextensive electrons, (a') Hydrogen plasma with superextensive electrons, (b) Argon plasma with Maxwellian electrons, (b') Hydrogen plasma with Maxwellian electrons.

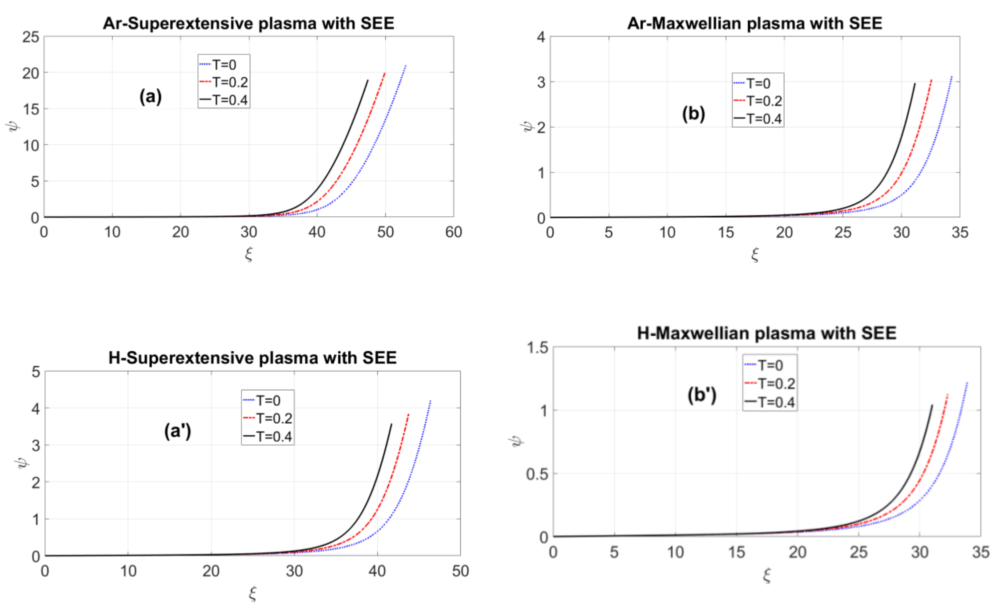

Fig. 4. Normalized potential versus ξ in superextensive and Maxwellian plasmas at different ion temperatures T with SEE: (a) Argon plasma with superextensive electrons, (a') Hydrogen plasma with superextensive electrons, (b) Argon plasma with Maxwellian electrons, (b') Hydrogen plasma with Maxwellian electrons.

4 Conclusion

The characteristics of thermal electropositive plasma sheath have been numerically analyzed in the presence of secondary electron emission produced by both positive ions and primary electrons. The numerical results obtained for the Maxwell-Boltzmann distribution (q = 1) were compared with those of the superextensive distribution (q < 1). On one hand, it was shown that in both argon and hydrogen plasmas, increasing q leads to a faster decrease of the electrostatic potential, a higher density of secondary electrons within the sheath, and a slightly lower value at the sheath edge. On the other hand, it was observed that independent of the primary electron distribution, the effect of positive ion temperature is more pronounced in lighter plasmas such as hydrogen compared to argon, especially when ion-induced SEE is taken into consideration. It was also shown that the influence of SEE due to ion bombardment on the sheath width is negligible. However, the sheath becomes wider for heavier ions and narrower when the positive ion temperature increases. This work may be relevant to fusion devices, including tokamaks and plasma processing applications where plasmas containing energetic electrons interact with emitting surfaces.

References

1. A.J. Perry, D. Vender, R.W. Boswell, The application of the helicon source to plasma processing. J. Vac. Sci. Technol. B **9**, 310–317 (1991). https://doi.org/10.1116/1.585611
2. A. Fruchtman, The thrust of a collisional-plasma source. IEEE Trans. Plasma Sci. **39**, 530–539 (2011). https://doi.org/10.1109/TPS.2010.2089067
3. G.M. McCracken, P.E. Stott, Plasma-surface interactions in tokamaks. Nucl. Fusion **19**, 889–898 (1979). https://doi.org/10.1088/0029-5515/19/7/004
4. M.S. Roslan, M.H. Jameel, A. Mohamad, A.F. Mat Zin, S.Z. Haider, N. Nayan, Plasma technology for solar cells, in *Energy From Plasma*, edited by A. Mohamad et al. (Woodhead Publishing, 2025), pp. 389–409
5. M.D. Campanell, Negative plasma potential relative to electron-emitting surfaces. Phys. Rev. E **88**, 033103 (2013). https://doi.org/10.1103/PhysRevE.88.033103
6. J.P. Sheehan, N. Hershkowitz, I.D. Kaganovich, H. Wang, Y. Raitses, E.V. Barnat, B.R. Weatherford, D. Sydorenko, Kinetic theory of plasma sheaths surrounding electron-emitting surfaces. Phys. Rev. Lett. **111**, 075002 (2013).
7. G.D. Hobbs, J.A. Wesson, Heat flow through a Langmuir sheath in the presence of electron emission. Plasma Phys. **9**, 85–94 (1967).
8. D. Sydorenko, A. Smolyakov, I. Kaganovich, Y. Raitses, Plasma-sheath instability in Hall thrusters due to periodic modulation of the energy of secondary electrons in cyclotron motion. Phys. Plasmas **15**, 053506 (2008). https://doi.org/10.1063/1.2918333
9. A.M. Capece, M.I. Patino, Y. Raitses, B.E. Koel, Secondary electron emission from lithium and lithium compounds. Appl. Phys. Lett. **109**, 011605 (2016).
10. S.F. Masoudi, S.S. Esmaeili, S. Jazavandi, Ion dynamics in plasma sheath under the effect of E×B and collisional forces. Vacuum **84**, 382–386 (2009).
11. J.-Y. Liu, Z.-X. Wang, X. Wang, Sheath criterion for a collisional sheath. Phys. Plasmas **10**, 3032–3034 (2003). https://doi.org/10.1063/1.1584048
12. X.-Y. Zhao, N. Xiang, J. Ou, D.-H. Li, B.-B. Lin, Sheath structure in plasma with two species of positive ions and secondary electrons. Chin. Phys. B **25**, 025202 (2016).
13. H. Amemiya, B.M. Annaratone, J.E. Allen, The double sheath associated with electron emission into a plasma containing negative ions. J. Plasma Phys. **60**, 81–93 (1998).
14. G.C. Das, B. Singha, J. Chutia, Characteristic behavior of the sheath formation in thermal plasma. Phys. Plasmas **6**, 3685–3689 (1999). https://doi.org/10.1063/1.873627
15. J.A.S. Lima, R. Silva Jr., J. Santos, Plasma oscillations and nonextensive statistics. Phys. Rev. E **61**, 3260–3266 (2000). https://doi.org/10.1103/PhysRevE.61.3260
16. C. Anteneodo, C. Tsallis, Breakdown of exponential sensitivity to initial conditions: Role of the range of interactions. Phys. Rev. Lett. **80**, 5313–5316 (1998).
17. E.G.D. Cohen, Statistics and dynamics. Physica A **305**, 19–26 (2002).
18. C. Tsallis, Possible generalization of Boltzmann-Gibbs statistics. J. Stat. Phys. **52**, 479–487 (1988). https://doi.org/10.1007/BF01016429
19. D.R. Borgohain, K. Saharia, K.S. Goswami, Behavior of plasma sheath with nonextensively distributed two-temperature electrons and isothermal ions. Phys. Plasmas **23**, 122113 (2016). https://doi.org/10.1063/1.4972072
20. A. Asserghine, F. Maaroufi, Behavior of thermal electropositive plasma near electron emitting surfaces. E3S Web Conf. **632**, 04001 (2025).

21. M. Sharifian, H.R. Sharifinejad, M. Borhani Zarandi, A.R. Niknam, Effect of q-non-extensive distribution of electrons on the plasma sheath floating potential. J. Plasma Phys. **80**, 607–618 (2014). https://doi.org/10.1017/S0022377813000688
22. M. Khoramabadi, H. Ghomi, P.K. Shukla, Numerical investigation of the ion temperature effects on magnetized DC plasma sheath. J. Appl. Phys. **109**, 073307 (2011). https://doi.org/10.1063/1.3569844